Title

Protective effect of human serum amyloid P on CCl4-induced acute liver injury in mice.

Journal

International journal of molecular medicine, 40(2)

ISSN

1107-3756

Authors

Cong, Min
Zhao, Weihua
Liu, Tianhui
et al.

Publication Date

2017-08-01

DOI

10.3892/ijmm.2017.3028

Peer reviewed

Protective effect of human serum amyloid P on CCl_4-induced acute liver injury in mice

MIN CONG[1], WEIHUA ZHAO[2], TIANHUI LIU[2], PING WANG[2], XU FAN[2], QINGLING ZHAI[2], XIAOLI BAO[2], DONG ZHANG[2], HONG YOU[2], TATIANA KISSELEVA[3], DAVID A. BRENNER[4], JIDONG JIA[2] and HUI ZHUANG[1]

[1]Department of Microbiology and Infectious Disease Center, School of Basic Medical Sciences, Peking University Health Science Center, Beijing 100191; [2]Liver Research Center, Beijing Friendship Hospital, Capital Medical University; Beijing Key Laboratory of Translational Medicine in Liver Cirrhosis and National Clinical Research Center of Digestive Diseases, Beijing 100050, P.R. China; Departments of [3]Surgery and [4]Medicine, UC San Diego, San Diego, La Jolla, CA 92093, USA

Received July 4, 2016; Accepted June 8, 2017

DOI: 10.3892/ijmm.2017.3028

Abstract. Human serum amyloid P (hSAP), a member of the pentraxin family, inhibits the activation of fibrocytes in culture and inhibits experimental renal, lung, skin and cardiac fibrosis. As hepatic inflammation is one of the causes of liver fibrosis, in the present study, we investigated the hepatoprotective effects of hSAP against carbon tetrachloride (CCl_4)-induced liver injury. Our data indicated that hSAP attenuated hepatic histopathological abnormalities and significantly decreased inflammatory cell infiltration and pro-inflammatory factor expression. Moreover, CCl_4-induced apoptosis in the mouse liver was inhibited by hSAP, as measured by terminal-deoxynucleotidyl transferase mediated nick-end labeling (TUNEL) assay and cleaved caspase-3 expression. hSAP significantly restored the expression of B cell lymphoma/leukemia (Bcl)-2 and suppressed the expression of Bcl-2-associated X protein (Bax) *in vivo*. The number of hepatocytes in early apoptosis stained with Annexin V was significantly reduced by 28-30% in the hSAP treatment group compared with the CCl_4 group, and the expression of Bcl-2 was increased, whereas the expression of Bax and cleaved caspase-3 were significantly inhibited in the hSAP pre-treatment group compared with the CCl_4 group. hSAP administration also inhibited the migration and activation of hepatic stellate cells (HSCs) in CCl_4-injured liver and suppressed the activation of isolated primary HSCs induced by transforming growth factor (TGF)-β1 *in vitro*. Collectively, these findings suggest that hSAP exerts a protective effect againts CCl_4-induced hepatic injury by suppressing the inflammatory response and hepatocyte apoptosis, potentially by inhibiting HSC activation.

Correspondence to: Dr Hui Zhuang, Department of Microbiology and Infectious Disease Center, School of Basic Medical Sciences, Peking University Health Science Center, 38 Xueyuan Road, Haidian, Beijing 100191, P.R. China
E-mail: zhuangbmu@126.com

Dr Jidong Jia, Liver Research Center, Beijing Friendship Hospital, Capital Medical University; Beijing Key Laboratory of Translational Medicine in Liver Cirrhosis and National Clinical Research Center of Digestive Diseases, 95 Yong-an Road, Xi-Cheng, Beijing 100050, P.R. China
E-mail: jiamd@263.net

Abbreviations: α-SMA, α-smooth muscle actin; Bax, Bcl-2-associated X protein; Bcl-2, B cell lymphoma/leukemia-2; CCl_4, carbon tetrachloride; HSCs, hepatic stellate cells; IL, interleukin; MCP, monocyte chemotactic protein; MIP, macrophage inflammatory protein; SAP, serum amyloid P; hSAP, human serum-derived SAP; TGF-β1, transforming growth factor-β1; TIMP-1, tissue inhibitor of metalloproteinases-1; TNF-α, tumor necrosis factor-α; TUNEL, terminal-deoxynucleotidyl transferase mediated nick end labeling

Key words: human serum amyloid P, carbon tetrachloride, inflammation, hepatocytes, apoptosis, hepatic stellate cells

Introduction

Liver injury is generally considered to be a result of exposure to high levels of environmental toxins and is associated with metabolic dysfunctions ranging from the transient elevation of liver enzymes to life-threatening hepatic fibrosis, liver cirrhosis and even hepatocellular carcinoma (1). Liver inflammation is commonly associated with hepatocyte necrosis and apoptosis (2). Apoptotic hepatocyte bodies can activate quiescent hepatic stellate cells (HSCs) and Kupffer cells, and these activated cell populations in turn promote inflammation and fibrogenesis (2). Activated HSCs also increase the production of inflammatory chemokines (3), the expression of adhesion molecules (4) and the presentation of antigens to T lymphocytes and natural killer T cells (5). These enhanced inflammation and immune responses can promote hepatocyte necrosis and apoptosis, and thereby strengthen and perpetuate the stimuli for fibrogenesis (6). The sustained suppression of inflammatory activity by eliminating the etiological agent (7-9) or by dampening the immune response (10,11) can halt and even reverse fibrotic progression. The success of current treatments for chronic liver inflammation in achieving anti-fibrotic effects can be measured by prolonged survival and possibly by the reduced occurrence of hepatocellular carcinoma (7,12,13).Therefore, hepatic inflammation is one of the causes of fibrosis, cirrhosis and hepatocellular carcinoma.

Serum amyloid P (SAP), a member of the pentraxin family of proteins, has been shown to inhibit fibrosis in a number of organ sites in preclinical animal models, in part due to the inhibition of the differentiation of circulating collagen I^+ cells (14,15). These cells have been demonstrated to be involved in the pathology associated with bleomycin-induced lung fibrosis (16). In previously published articles conducted using the bleomycin model of lung fibrosis in mice and rats (15), intra-peritoneal injections of purified rat SAP (rSAP) into rats, or purified mouse SAP (mSAP) into mice, significantly reduced fibrocyte and macrophage recruitment to the lungs, as well as myofibroblast activation and collagen deposition. SAP injections also reduced bleomycin-induced leukocyte infiltration into rat lungs (15) and transforming growth factor (TGF)-β1-induced lung inflammation in mice (17). As liver fibrosis shares similar biological signals with fibrosis in a number of different organ models, and as hepatic fibrosis commonly follows chronic inflammation (6), we hypothesized that human serum amyloid P (hSAP) may exert protective effects on hepatocytes during hepatic inflammation/fibrosis.

Promedior, Inc. (Malvern, PA, USA) recently developed PRM-151, a recombinant form of hSAP. Cross-species comparison assays *in vitro* demonstrated comparable efficacy of human serum-derived SAP (hSAP), recombinant hSAP (rhSAP) and mSAP or rSAP for inhibiting mouse or rat monocytes from fibrocyte differentiation. Additionally, cross-species comparison assays *in vitro* demonstrated comparable efficacy for hSAP and rhSAP at inhibiting human and cynomolgus monkey fibrocyte differentiation (18). Taken together, these results confirmed the conservation of biological function across species. In this study, we investigated the protective effects of hSAP against carbon tetrachloride (CCl_4)-induced acute liver injury in mice, including hepatoprotective and anti-inflammatory effects in acute liver injury, as well as the potential of hSAP to inhibit the migration and activation of HSCs.

Materials and methods

hSAP. hSAP is formulated in a P5SP vehicle (10 mM sodium phosphate, 5% (w/v) sorbitol and 0.01% (w/v) polysorbate 20, pH 7.5) at a concentration of 1.25 mg/ml. The drug was shipped frozen and was stored at -20˚C until initial use. The frozen drug was gently thawed, and vigorous agitation was avoided.

Animal use and care. Male C57BL/6 8-week-old mice, weighing 20.0±2 g, were purchased from Vital River Laboratories (Beijing, China). The mice were maintained in a pathogen-free environment in the animal facilities at Beijing Friendship Hospital. All protocols were approved by the Beijing Friendship Hospital Animal Care and Ethics Committee (13-2006).

The mice were randomly allocated into 7 groups (n=8 in each group). Group I (normal) was administered the same volume of solvent (olive oil) by intraperitoneal injection. In the second and third groups (CCl_4-exposed groups, 24 and 48 h), acute liver injury was induced by the administration of a single intraperitoneal dose of CCl_4 (10 μl/g) dissolved in olive oil (1:7). In the fourth and fifth groups (hSAP-treated + CCl_4-exposed groups, 24 and 48 h), the mice first received an intravenous dose of hSAP (12.5 mg/kg); they were then intraperitoneally injected with a single dose of CCl_4 2 h later, in the same manner as the CCl_4-exposed group. In the sixth and seventh groups (vehicle-treated + CCl_4-exposed group, 24 and 48 h), the mice received the same procedure, but received the vehicle at the same volume as hSAP. At 24 h (24 h group) and 48 h (48 h group) after the CCl_4 injection, the mice were sacrificed under anesthesia. Some liver tissues were fixed in 4% paraformaldehyde for subsequent histological examination and some liver tissues were stored at -80˚C for further experiments.

Histological examination and terminal-deoxynucleotidyl transferase mediated nick-end labeling (TUNEL) assay. Liver samples were fixed in 4% paraformaldehyde, paraffin embedded and sectioned. Hematoxylin and eosin (H&E) staining was performed by Wuhan Goodbio Technology Co., Ltd. (Wuhan, China). Necrotic hepatocytes show distinctive cytoplasmic eosinophilia, abnormal sizes and contours and nuclear pyknosis and karyorrhexis. Five high-power fields at x200 magnification were randomly selected, and the degree of cellular death due to necrosis was analyzed semiquantitatively using image analysis with the National Institutes of Health image program (ImageJ) following the user's guide (http://imagej.net/docs/guide). Immunohistochemistry was performed on paraffin-embedded mouse liver sections using the specific antibody for CD45 (GB11066; Wuhan Goodbio Technology Co., Ltd.), desmin (D93F5; Cell Signaling Technology, Danvers, MA, USA) and α-smooth muscle actin (α-SMA; ab5694; Abcam, Cambridge, MA, USA) to detect inflammatory cells and HSCs in livers. The negative control was the replacement of primary antibody with non-immune serum. For the detection of cell apoptosis, TUNEL assay was performed following the manufacturer's instructions (11684795910; Roche, Indianapolis, IN, USA). In each tissue specimen, 5 high-power fields at x200 magnification were randomly selected, and the percentage of positive cells was quantified using ImageJ software.

Primary HSC isolation and cell culture. Primary HSCs were isolated from 3 wild-type C57BL/6 8-week-old mice by a 2-step collagenase-pronase perfusion of mouse livers followed by 8.2% Nycodenz (Accurate Chemical and Scientific Corp., Westbury, NY, USA). Two-layer discontinuous density gradient centrifugation was performed as previously described (19). Isolated HSCs were cultured in Dulbecco's modified Eagle's medium (DMEM; Gibco, Grand Island, NY, USA) containing 10% fetal bovine serum. For HSC activation experiments *in vitro*, the cells were cultured overnight in serum-free medium prior to the experiments. The HSCs were then cultured with hSAP (30 μg/ml) or vehicle for 4 h before stimulation with TGF-β1 (10 ng/ml for 24 h; PeproTech, Rocky Hill, NJ, USA) (20). Following 24 h of incubation, all cells were harvested for further experiments.

Dual-fluorescent immunohistochemistry and Oil Red O staining for the identification of isolated primary HSCs. Isolated primary HSCs seeded on sterile slides were fixed with 4% paraformaldehyde and permeated with 0.1% Triton X-100. Non-specific binding was blocked with 1% bovine serum albumin for 30 min. The cells were then incubated with primary antibodies against desmin (D93F5; Cell Signaling Technology) at 4˚C overnight, followed by secondary

Table I. Primers used for quantitative PCR.

Gene	Forward primer (5'→3')	Reverse primer (5'→3')
IL-1β	GGT CAA AGG TTT GGA AGC AG	TGT GAA ATG CCA CCT TTT GA
IL-6	ACCAGAGGAAATTTTCAATAGGC	TGATGCACTTGCAGAAAACA
TNF-α	AGGGTCTGGGCCATAGAACT	CCACCACGCTCTTCTGTCTAC
MCP-1	ATTGGGATCATCTTGCTGGT	CCTGCTGTTCACAGTTGCC
MIP-2	TCCAGGTCAGTTAGCCTTGC	CGGTCAAAAAGTTTGCCTTG
CD11b	GTTTGTTGAAGGCATTTCCC	ATTCGGTGATCCCTTGGATT
Bcl-2	CTT TCT GCT TTT TAT TTC ATG AGG	CAG AAG ATC ATG CCG TCC TT
Bax	GAT CAG CTC GGG CAC TTT AG	TTG CTG ATG GCA ACT TCA AC
α-SMA	GTTCAGTGGTGCCTCTGTCA	ACTGGGACGACATGGAAAAG
TIMP-1	AGGTGGTCTCGTTGATTTCT	GTAAGGCCTGTAGCTGTGCC
β-actin	ATGGAGGGGAATACAGCCC	TTCTTTGCAGCTCCTTCGTT

IL, interleukin; TNF-α, tumor necrosis factor-α; MCP-1, monocyte chemotactic protein-1; MIP-2, macrophage inflammatory protein-2; Bcl-2, B cell lymphoma/leukemia-2; Bax, Bcl-2 associated X protein; α-SMA, α-smooth muscle actin; TIMP-1, tissue inhibitor of metalloproteinases-1.

antibodies for 40 min. Nuclei were counterstained with 4',6-diamidino-2-phenylindole (DAPI) (Invitrogen, Carlsbad, CA, USA) for 5 min. To detect lipid droplets in freshly isolated HSCs, the cells were fixed in ice-cold 4% paraformaldehyde for 20 min at room temperature prior to incubation for 10 min in a saturated solution of Oil Red O (G1016; Wuhan Goodbio Technology Co., Ltd.) in isopropanol. The slides were counterstained with Mayer's haematoxylin. Images were captured using a fluorescence microscope (Nikon, Tokyo, Japan).

Hepatocyte cell line and apoptosis assay. To avoid the adverse effects of hepatocyte injury produced during perfusion on the detection of cell death, we used the mouse hepatocyte cell line, NCTC 1469 (Cell Resource Center, Chinese Academy of Medical Sciences and Peking Union Medical College) to detect the potential protective effects of hSAP on hepatocyte death induced by CCl_4. NCTC 1469 cells were cultured with hSAP (30 μg/ml) or the vehicle for 4 h prior to stimulation with CCl_4 (2.5 mM for 4 h), as previously described (21). We used DMSO to dissolve CCl_4 and DMSO is the vehicle control. Apoptosis was assessed using a PE Annexin V apoptosis detection kit (559763; BD Pharmingen, San Jose, CA, USA) following the manufacturer's instructions. The cells were analyzed with a FACSCalibur flow cytometer (Becton-Dickinson, San Jose, CA, USA), and the cells considered viable were PE-negative and 7-AAD-negative. Cells in early apoptosis were PE Annexin V-positive and 7-AAD-negative, and cells in late apoptosis or dead were both PE Annexin V-positive and 7-AAD-positive.

RNA extraction, reverse transcription and quantitative PCR. Total RNA was extracted from the cell pellets or tissues using TRIzol reagent (Invitrogen) according to the manufacturer's instructions. The reverse transcription reaction was performed using a high capacity cDNA reverse transcription kit (4375575; Applied Biosystems, Foster City, CA, USA). The cDNA was subjected to PCR in the presence of SYBR-Green dye, with the ABI power SYBR-Green PCR Master Mix kit (4367659; Applied Biosystems). Quantitative PCR was performed on a 7500 real-time PCR instrument (Applied Biosystems). Mouse primers were designed using Primer 3 and were synthesized by SBS Genetech Co., Ltd. (Beijing, China) (Table I). The relative mRNA levels of genes were calculated using the $2^{-\Delta\Delta Ct}$ formula, and mouse β-actin was used as a housekeeping gene. All experiments were performed independently 3 times, and the average was used for comparison.

Protein extraction and western blot analysis. The preparation of protein extracts from frozen livers or isolated cells, electrophoresis, and subsequent blotting were performed as previously described (22,23). We incubated the blots with primary antibodies to B cell lymphoma/leukemia (Bcl)-2 (1:1,000; 50E3), Bcl-2-associated X protein (Bax, 1:1,000; 2772), cleaved caspase-3 (1:1,000; 5A1E) (all from Cell Signaling Technology), α-SMA (1:2,000; 5694), tissue inhibitor of metalloproteinases (TIMP)-1 (1:1,000; 38978) (both from Abcam) and β-actin (1:5,000; A1978; Sigma, St. Louis, MO, USA) at 4˚C overnight. This was followed by the addition of the appropriate horseradish peroxidase-conjugated secondary antibody (1:10,000; ZB2301 or ZB2306; ZSGB Bio, Beijing, China) and incubation for 60 min and specific antibody-antigen complexes were detected with the ECL western blot detection kit (Pierce, Rockford, IL, USA). All experiments were performed independently at least 3 times, and protein expression was quantified by densitometric analysis of immunoblots using Quantity One software (Thermo Fisher Scientific, Waltham, MA, USA).

Statistical analysis. Data are expressed as the means ± standard deviation (SD). Two-group comparisons were conducted using the Student's t-test, and comparisons of the means of 3 or more groups were performed by ANOVA. A value of $P<0.05$ was considered to indicate a statistically significant difference.

Results

Effects of hSAP pre-treatment on the histopathological changes in the livers of mice. H&E staining of the liver tissue sections revealed severe and diffuse centrilobular necrosis in the mice at 24 h following CCl_4 administration. By contrast,

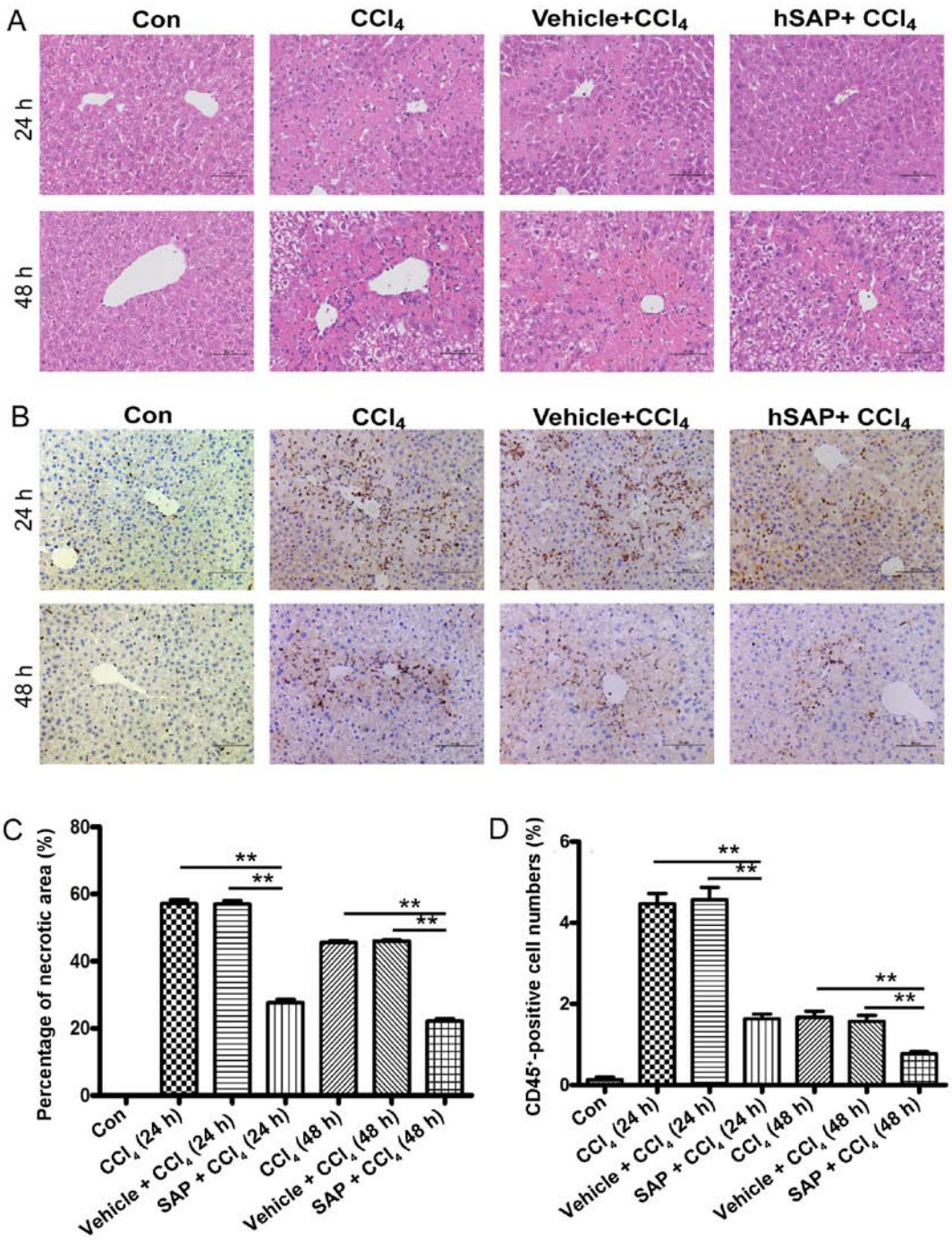

Figure 1. Human serum amyloid P (hSAP) alleviates liver inflammatory reactions in mice with carbon tetrachloride (CCl_4)-induced liver injury. Mice were treated intravenously with hSAP (12.5 mg/kg) or the vehicle for 2 h. The mice were then subcutaneously injected with 12.5% CCl_4 for 24 or 48 h to develop an acute liver injury. (A) Liver sections from animal models were subjected to hematoxylin and eosin staining to detect histopathological changes (x200 magnification). (B) Liver sections from animal models were subjected to immunohistochemical staining with CD45 for the detection of infiltrating inflammatory cells. (C) The percentage of necrotic area of 5 high-power fields at x200 magnification is shown. (D) The number of CD45-positive cells/total number of cells x100% of 5 high-power fields at x200 magnification is shown. Values are expressed as the means ± SD in each group. $^{**}P<0.01$, n=8 mice/group. Scale bar, 50 μm.

only spotty necrosis of the hepatocytes was found in the livers of CCl_4-challenged mice pre-treated with hSAP. In addition, less inflammatory cell infiltration was observed in the hSAP + CCl_4 group compared with the CCl_4 group and the vehicle + CCl_4 group. Diffuse centrilobular necrosis and inflammatory reactions were decreased in each group 48 h after the CCl_4 administration; however, hSAP administration continued to decrease the necrotic area and inflammatory reaction at this time point (Fig. 1A and C).

hSAP pre-treatment inhibits CCl_4-induced inflammatory cell infiltration and pro-inflammatory factors, and chemokine expression. CD45 cell surface antigen is a transmembrane protein expressed by all nucleated cells of hematopoietic origin, apart from erythrocytes and platelets (24). In this study, we used this marker to lable inflammatory cells in the injured liver. Immunohistochemical staining revealed that the number of CD45-positive cells accumulating in the liver sections was decreased by hSAP treatment compared with that of the CCl_4

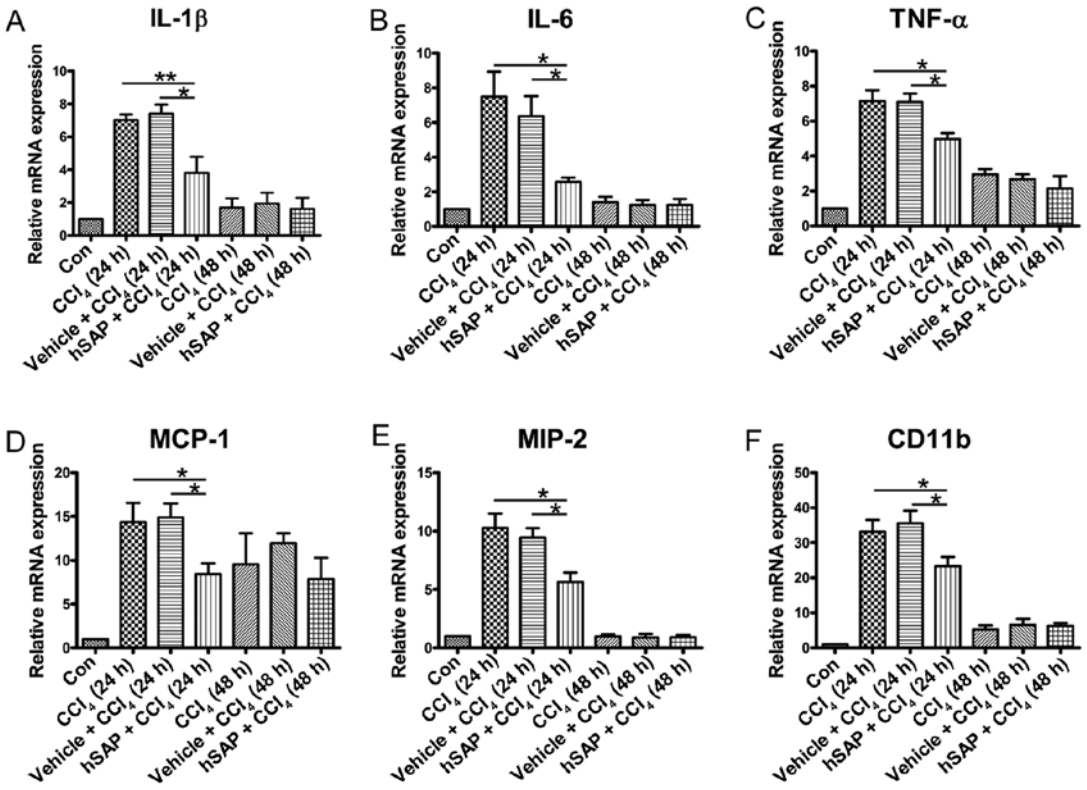

Figure 2. Human serum amyloid P (hSAP) pre-treatment inhibits carbon tetrachloride (CCl_4)-induced pro-inflammatory factors and chemokine expression in mouse livers. The mRNA expression of (A) interleukin (IL)-1β, (B) IL-6, (C) tumor necrosis factor (TNF)-α, (D) monocyte chemotactic protein (MCP)-1, (E) MIP-2 and (F) CD11b from a whole-liver sample was detected using quantitative PCR. β-actin was used as a loading control. *P<0.05 and **P<0.01, n=8 mice/group. The results shown represent 3 independent experiments.

and vehicle + CCl_4 groups (P<0.01; Fig. 1B and D). Exposure to CCl_4 significantly increased the hepatic interleukin (IL)-1β, IL-6 and tumor necrosis factor (TNF)-α mRNA expression levels compared with those of the normal group, suggesting the induction of a severe inflammatory response. However, the pre-administration of hSAP suppressed the mRNA expression of hepatic IL-1β, IL-6 and TNF-α (Fig. 2A-C). In addition, the levels of chemokines that regulate inflammation, such as monocyte chemotactic protein (MCP)-1 and macrophage inflammatory protein (MIP)-2, were also detected. High expression levels of MCP-1 and MIP-2 were observed in the CCl_4 and vehicle + CCl_4 groups, whereas hSAP administration down-regulated the expression of these chemokines (Fig. 2D and E). To confirm the inflammatory infiltration, we detected CD11b (a biomarker for neutrophils) expression in the liver. CD11b expression in the liver sections was decreased by hSAP treatment compared with the injury group (Fig. 2F). The levels of all pro-inflammatory factors and chemokine expression in the 24-h group were higher than those in the 48-h group, indicating that acute liver injury induced by CCl_4 reached a peak value at 24 h after CCl_4 administration.

hSAP pre-treatment decreases CCl_4-induced apoptosis in vivo. Previous studies have reported severe hepatocyte apoptosis in CCl_4-induced acute liver injury (25,26). In this study, to clarify whether the effect of hSAP on acute liver injury was primarily due to its inhibitory effect on hepatocyte apoptosis, we performed TUNEL staining to assess the protective ability of hSAP against CCl_4-induced hepatocyte apoptosis. The analysis of cleaved caspase-3 expression in the liver also revealed that the pre-administration of hSAP inhibited the increased apoptosis induced by exposure to CCl_4 (Fig. 3A, B and D). To determine the mechanisms underlying the anti-apoptotic effects of hSAP, the expression of the apoptosis-related genes, Bcl-2 and Bax, in hepatocytes was detected using quantitative PCR and western blot analysis. The pre-administration of hSAP significantly upregulated the expression levels of Bcl-2 and significantly downregulated the expression levels of Bax compared with those in the model group (Fig. 3C and D). The expression of Bcl-2, Bax and cleaved caspase-3 exhibited a significant difference in the hSAP pre-treatment group at 24 h following the CCl_4 administration compared with the model group (P<0.05 or P<0.01).

hSAP pre-treatment decreases the CCl_4-induced apoptosis of hepatocytes in vitro. To confirm the hepatocyte protective effects of hSAP, NCTC 1469 cells were cultured with hSAP (30 μg/ml) or the vehicle for 4 h prior to stimulation with CCl_4 (2.5 mM). Four hours later, the cells were collected, and cell death was detected using an apoptosis detection kit. The number of cells in early apoptosis stained with Annexin V was significantly reduced by 28-30% in the hSAP treatment group compared with the CCl_4 group (13.4±0.9 vs. 18.5±1.5%) (Fig. 4A). The expression of Bcl-2 was increased, whereas the expression levels of Bax and cleaved caspase-3 were significantly inhibited in the hSAP pre-treatment group compared with the CCl_4 group (P<0.01), indicating that hSAP has a direct anti-apoptotic function on hepatocytes exposed to CCl_4 (Fig. 4B-D).

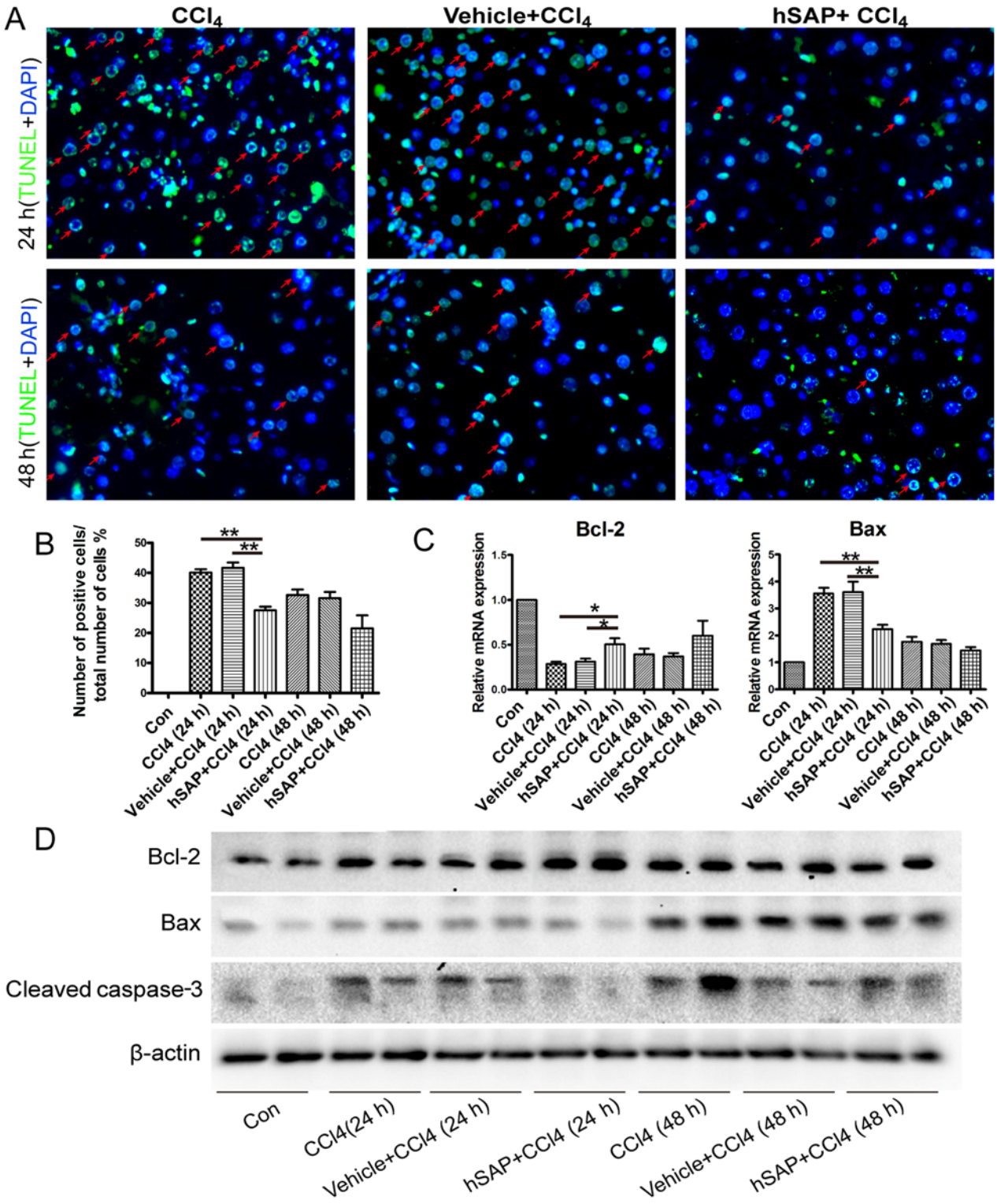

Figure 3. Human serum amyloid P (hSAP) pre-treatment inhibits carbon tetrachloride (CCl_4)-induced apoptosis *in vivo*. (A) Liver sections were subjected to a terminal-deoxynucleotidyl transferase mediated nick-end labeling (TUNEL) assay to detect cell apoptosis (x400 magnification). Apoptotic hepatocytes were stained by green fluorescence. (B) The apoptotic index (number of positive cells/total number of cells x100%) of 5 high-power fields at x400 magnification is shown. (C) The mRNA expression of B cell lymphoma/leukemia-2 (Bcl-2) and Bcl-2 associated X protein (Bax) from a whole-liver sample was detected by real-time PCR. β-actin was used as a loading control. (D) The protein level of Bcl-2, Bax and cleaved caspase-3 from a whole liver sample was detected by western blot analysis. *P<0.05 and **P<0.01, n=8 mice/group. The results shown represent 3 independent experiments.

hSAP inhibits the migration and activation of HSCs in vivo. As activated HSCs secrete high levels of MCP-1 and MCP-1 in turn can promote the migration and positioning of HSCs (27,28), we further detected the migration of HSCs in injured livers. Although aggregated HSCs were found around the necrotic area at 24 and 48 h following the CCl_4 administration, fewer HSCs migrated to these areas following hSAP administration, as confirmed by desmin staining (P<0.05; Fig. 5A and C).

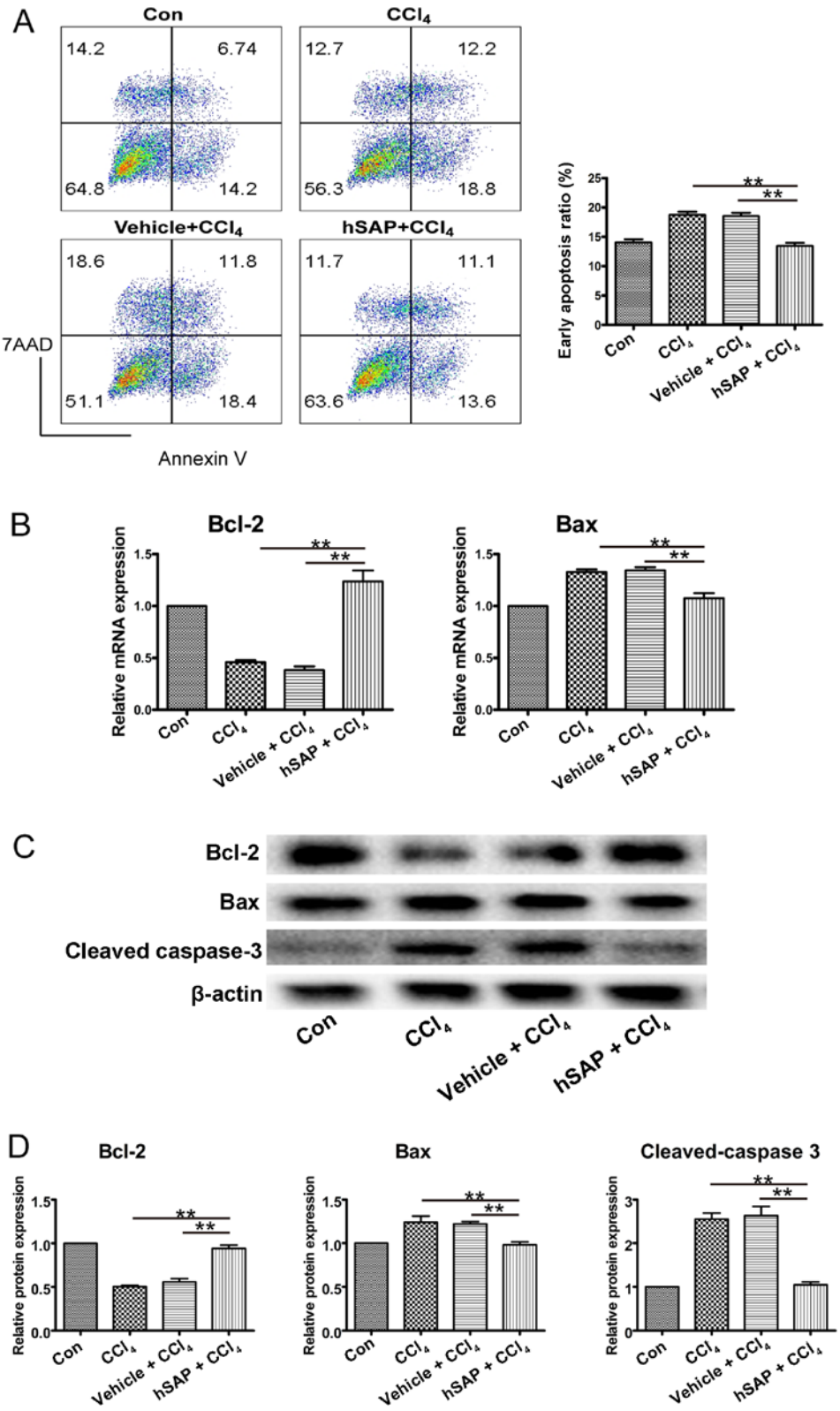

Figure 4. Human serum amyloid P (hSAP) pre-treatment decreases the carbon tetrachloride (CCl_4)-induced apoptosis of hepatocytes *in vitro*. NCTC 1469 cells were pre-treated with 30 μg/ml hSAP or the vehicle for 4 h and were then incubated with CCl_4 (2.5 mM) for 4 h. (A) Cells were trypsinized and stained with Annexin V and 7-AAD followed by analysis with flow cytometry. Early apoptotic cells (Annexin V positive and 7-AAD negative) are in the right lower quadrant. Late apoptotic or necrotic cells are in the right upper quadrant. The ratio of early apoptotic cells to total cells x100% is shown. (B) The mRNA expression of B cell lymphoma/leukemia-2 (Bcl-2) and Bcl-2 associated X protein (Bax) from cells was detected using quantitative PCR. β-actin was used as a loading control. (C) The protein level of Bcl-2, Bax and cleaved caspase-3 from cells was detected by western blot analysis. (D) The expression levels of Bcl-2, Bax and cleaved caspase-3 were normalized to β-actin. $^{**}P<0.01$. The results shown represent 3 independent experiments.

Subsequently, we used α-SMA, a biomarker of activated HSCs, to detect the activation of HSCs in the injured liver. Although there were a limited number of activated HSCs in each group at 24 h following the CCl_4 administration, immunostaining

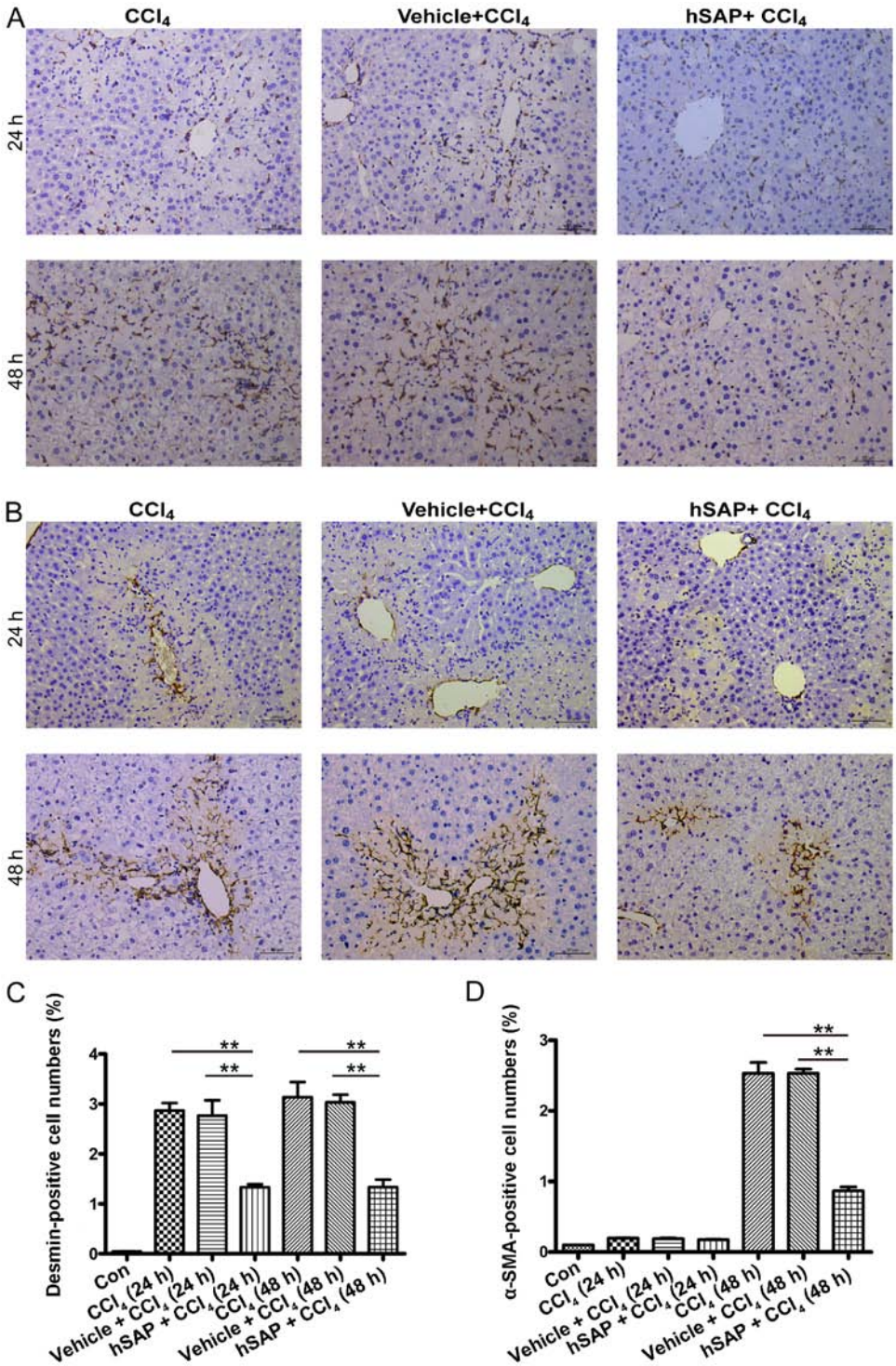

Figure 5. Human serum amyloid P (hSAP) inhibits the infiltration and activation of hepatic stellate cells (HSCs) *in vivo*. (A) Liver sections from animal models were subjected to immunohistochemical staining with desmin for the detection of infiltrating HSCs, and the number of desmin positive cells/total number of cells x100% of 5 high-power fields at x200 magnification is shown (C). (B) Liver sections from animal models were subjected to immunohistochemical staining with α-smooth muscle actin (α-SMA) for the detection of activated HSCs, and the number of α-SMA positive cells/total number of cells x100% of 5 high-power fields at x200 magnification is shown (D). $^{**}P<0.01$, n=8 mice/group. Scale bar, 50 μm.

of the tissue sections for α-SMA expression revealed intense staining patterns around the damaged hepatocytes in the mice from the CCl_4 and the vehicle + CCl_4 groups 48 h following the CCl_4 administration. The administration of hSAP resulted in approximately 65% decreased positive staining in the sinusoids, demonstrating fewer activated HSCs following hSAP treatment (Fig. 5B and D).

hSAP inhibits the TGF-β1-induced activation of HSCs in vitro. CCl_4 is a hepatotoxin, which causes the apoptosis of damaged hepatocytes. Apoptotic hepatocytes release factors that activate Kupffer cells, the major source of TGF-β1. Quiescent HSCs are induced by TGF-β1 to transdifferentiate into myofibroblasts that secrete extracellular matrix (2). Based on the observed weaker activation of HSCs in the injured liver of hSAP-treated

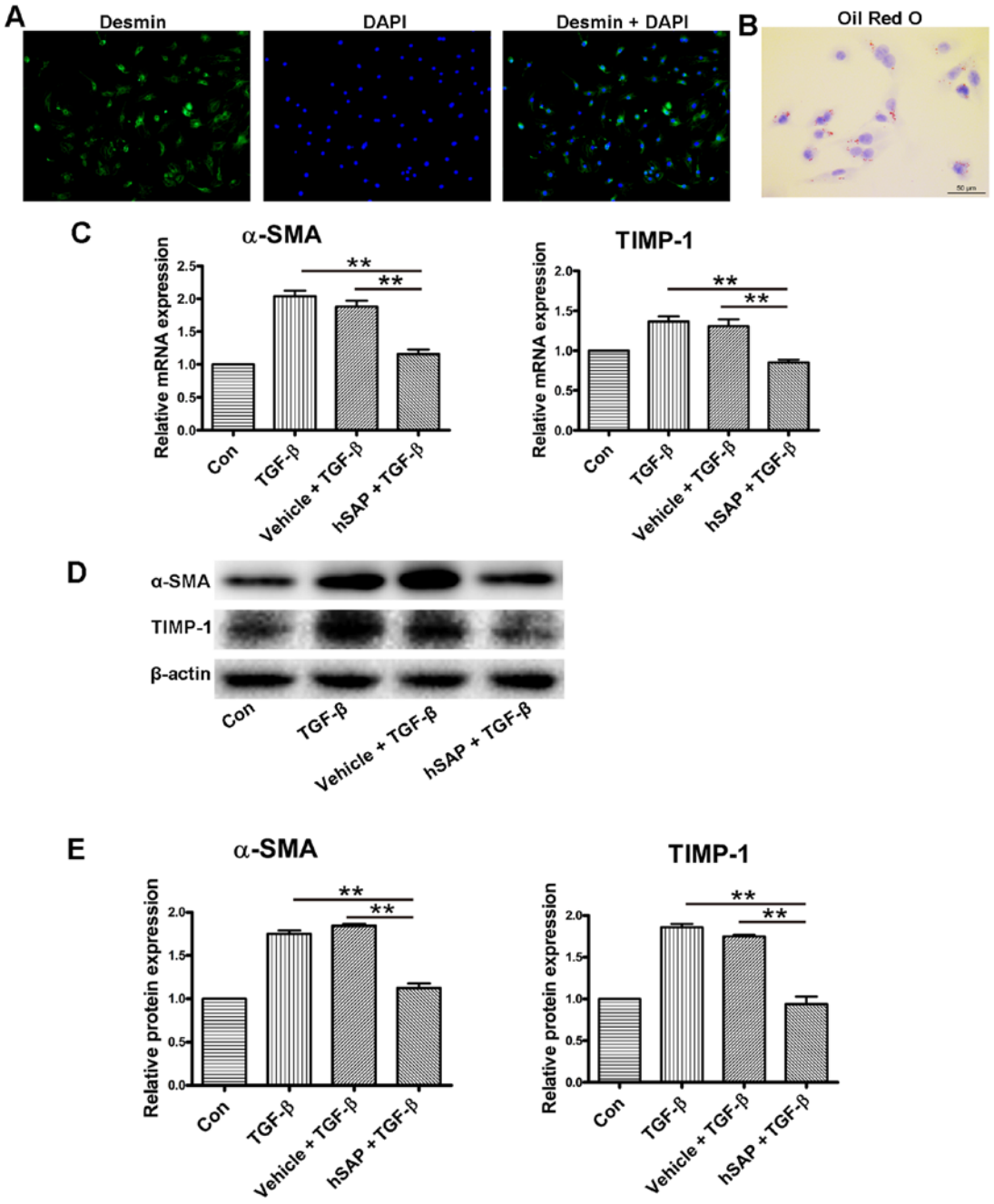

Figure 6. Human serum amyloid P (hSAP) inhibits the transforming growth factor (TGF)-β1-induced activation of hepatic stellate cells (HSCs) *in vitro*. (A) The purity of isolated HSCs was assessed by immunoflurescence staining of desmin and Oil Red O staining (B). (C) Isolated primary HSCs were cultured with hSAP (30 μg/ml) or the vehicle for 4 h before stimulation with TGF-β1 (10 ng/ml for 24 h). The mRNA expression of α-smooth muscle actin (α-SMA) and tissue inhibitor of metalloproteinases (TIMP)-1 was detected by quantitative PCR. β-actin was used as a loading control. (D) The protein levels of α-SMA and TIMP-1 were detected by western blot analysis. (E) The expression levels of α-SMA and TIMP-1 were normalized to β-actin. **P<0.01. The results shown represent 3 independent experiments. Scale bar, 50 μm.

mice, we wished to elucidate whether hSAP inhibits the TGF-β1-induced activation of HSCs directly *in vitro*. Primary HSCs were isolated from wild-type C57BL/6 mice, and the purity was >98%, as assessed by desmin immunofluorescence staining and Oil Red O staining (Fig. 6A and B). Following 24 h of incubation with TGF-β1, the isolated HSCs exhibited a significantly lower activation in the 30 μg/ml hSAP treatment group. The mRNA and protein levels of α-SMA and TIMP-1 in the hSAP treatment group were significantly reduced compared with those in the TGF-β1 group (Fig. 6C-E).

Discussion

Carbon tetrachloride is a widely used hepatotoxin to establish animal models for evaluating the hepatoprotective activities of drugs (29). In the present study, mice injected with CCl_4 exhibited characteristics of acute liver injury, including distorted hepatic parenchyma, inflammatory cell infiltration and hepatocyte necrosis (visualized by H&E staining). However, pre-treatment with hSAP significantly decreased the CCl_4-induced histopathological changes in the livers. These

findings indicate that hSAP can exert protective effects against CCl_4-induced liver damage.

The inflammatory response is involved in the process of CCl_4-induced acute liver injury (30). The traditional inflammatory response is characterized as a complex reaction to an injuring agent that involves the loss of vascular wall integrity, the effusion of inflammatory cells, the activation of leukocytes and their extravasations, and the release of pro-inflammatory cytokines, such as TNF-α, IL-6 and IL-1β (31,32). In this study, the CD45 antibody was used to stain inflammatory cells in liver sections, and we found that hSAP treatment significantly reduced inflammatory infiltration compared with the injury group. Exposure to CCl_4 significantly upregulated the expression of pro-inflammatory cytokines (TNF-α, IL-6 and IL-1β), chemokines (MCP-1 and MIP-2) and CD11b (marker of neutrophil activation) in injured mouse livers. However, the pre-administration of hSAP markedly inhibited the upregulation of these pro-inflammatory cytokines, chemokines and leukocyte infiltration. These results suggested that hSAP can meliorate liver injury caused by CCl_4 by inhibiting the inflammatory response.

Previous studies have demonstrated that hepatocyte apoptosis can be triggered by CCl_4 (25,26). In this study, the rate of apoptosis evaluated by TUNEL staining was significantly increased in the CCl_4 group, which was decreased by the pre-administration of hSAP. To investigate whether hSAP treatment modulates the molecular mechanisms involved in apoptosis, we detected the expression of apoptosis-related molecules, particularly Bcl-2 (anti-apoptotic protein), Bax (pro-apoptotic protein) and caspase-3. The present study demonstrated that the pre-administration of hSAP suppressed the upregulation of Bax expression, inhibited the activation of caspase-3, and restored Bcl-2 expression which was decreased by CCl_4. The result that the mRNA expression of Bax reached a peak value at 24 h following CCl_4 administration, whereas Bax and cleaved-caspase-3 protein bands in the western blots were far denser at 48 h, could partially be explained by the timeline difference between the regulation of mRNA and protein expression. Our *in vitro* experiments also confirmed that hSAP significantly reduced the CCl_4-induced early apoptotic rate in hepatocytes by regulating the expression of the apoptosis-related proteins, Bax and Bcl-2.

Several studies have proposed that the phagocytosis of apoptotic bodies by HSCs links cell death to HSC activation, showing increased HSC activation and survival after the phagocytosis of apoptotic bodies *in vitro* (33-35). DNA from apoptotic hepatocytes can provide a stop signal to mobile HSCs when they reach an area of apoptotic hepatocytes and induce a stationary phenotype-associated upregulation of collagen production (36). Apoptotic body engulfment in HSCs also stimulates TGF-β1 expression and induces collagen I, indicating a fibrogenic response (33). In this study, the immunohistochemical staining of desmin (a biomarker for HSCs) and α-SMA (a biomarker for activated HSCs) showed that the pre-administration of hSAP inhibited the migration and activation of HSCs to the injured liver site and may be mediated by less apoptotic hepatocyte DNA in hSAP-pre-treated livers.

The short pentraxin, SAP, was recently described to reduce fibrosis in a number of different organ models, including pulmonary, renal, cardiac and oral submucous fibrosis, partially through the inhibition of fibrocyte and macrophage accumulation and activation in the injured organ (15,17,37-40). It has been demonstrated that the anti-fibrotic effects of SAP in TGF-β1-induced lung fibrosis are mediated through the modulation of monocyte responses (17), and that SAP also inhibits fibrosis through Fcγ receptor (FcγR)-dependent monocyte-macrophage regulation (37). HSCs are the main cell type responsible for liver fibrosis, and TGF-β1 is the most potent cytokine that can promote the activation of HSCs (2). In this study, to determine whether hSAP inhibits the activation of HSCs directly, we isolated primary HSCs from normal mouse liver and incubated these primary HSCs with or without hSAP and with TGF-β1 stimulation. Although TGF-β1 activated HSCs by upregulating the expression of α-SMA and TIMP-1, the mRNA and protein levels of these profibrogenic genes in the hSAP treatment group were significantly reduced by 43-45% compared with the control group. It has been shown that hSAP serves as a ligand for activating FcγRs and downregulates the activation of monocytes and macrophages (37). Primary rat HSCs express FcγRs (41), suggesting that hSAP may also bind directly to HSCs via FcRs. Rat hepatocytes may express MHC class I-related Fc receptor for IgG (42). For our *in vitro* experiment, we hypothesized that SAP could act on hepatocytes and HSCs by binding between SAP and FcγRs. Additional studies are required to fully investigate the mechanism through which hSAP inhibits the activation of HSCs.

In the present study, we demonstrated that hSAP has a strong anti-inflammatory and hepatoprotective effect in CCl_4-induced acute liver injury in mice, most likely through the combined effects of inhibiting leukocyte infiltration, inflammatory cytokine expression and hepatocyte apoptosis. hSAP may also inhibit HSCs activation directly or indirectly due to fewer apoptotic hepatocytes. Based on the intimate association between inflammation and fibrosis, the important role of HSCs in fibrogenesis and the inhibitory effects of hSAP on HSC activation, hSAP may also affect the development of liver fibrosis. Further studies are required to evaluate the role of SAP in liver fibrosis *in vitro* and *in vivo*.

Acknowledgements

We would like to thank Promedior, Inc. for providing hSAP. This study was supported by grants from the National Natural Science Foundation of China (no. 81570542), the Natural Science Foundation of Beijing Municipality (no. 7142043), and the Beijing Health System Talents Plan (no. 2013-3-057).

References

1. Reuber MD and Glover EL: Cirrhosis and carcinoma of the liver in male rats given subcutaneous carbon tetrachloride. J Natl Cancer Inst 44: 419-427, 1970.
2. Lee UE and Friedman SL: Mechanisms of hepatic fibrogenesis. Best Pract Res Clin Gastroenterol 25: 195-206, 2011.
3. Schwabe RF, Bataller R and Brenner DA: Human hepatic stellate cells express CCR5 and RANTES to induce proliferation and migration. Am J Physiol Gastrointest Liver Physiol 285: G949-G958, 2003.
4. Hellerbrand SC, Wang SC, Tsukamoto H, Brenner DA and Rippe RA: Expression of intracellular adhesion molecule 1 by activated hepatic stellate cells. Hepatology 24: 670-676, 1996.
5. Winau F, Hegasy G, Weiskirchen R, Weber S, Cassan C, Sieling PA, Modlin RL, Liblau RS, Gressner AM and Kaufmann SH: Ito cells are liver-resident antigen-presenting cells for activating T cell responses. Immunity 26: 117-129, 2007.

6. Czaja AJ: Hepatic inflammation and progressive liver fibrosis in chronic liver disease. World J Gastroenterol 20: 2515-2532, 2014.
7. Mallet V, Gilgenkrantz H, Serpaggi J, Verkarre V, Vallet-Pichard A, Fontaine H and Pol S: Brief communication: The relationship of regression of cirrhosis to outcome in chronic hepatitis C. Ann Intern Med 149: 399-403, 2008.
8. Kweon YO, Goodman ZD, Dienstag JL, Schiff ER, Brown NA, Burchardt E, Schoonhoven R, Brenner DA and Fried MW: Decreasing fibrogenesis: An immunohistochemical study of paired liver biopsies following lamivudine therapy for chronic hepatitis B. J Hepatol 35: 749-755, 2001.
9. Lau DT, Kleiner DE, Park Y, Di Bisceglie AM and Hoofnagle JH: Resolution of chronic delta hepatitis after 12 years of interferon alfa therapy. Gastroenterology 117: 1229-1233, 1999.
10. Czaja AJ and Carpenter HA: Decreased fibrosis during corticosteroid therapy of autoimmune hepatitis. J Hepatol 40: 646-652, 2004.
11. Mohamadnejad M, Malekzadeh R, Nasseri-Moghaddam S, Hagh-Azali S, Rakhshani N, Tavangar SM, Sedaghat M and Alimohamadi SM: Impact of immunosuppressive treatment on liver fibrosis in autoimmune hepatitis. Dig Dis Sci 50: 547-551, 2005.
12. Lok AS, Everhart JE, Wright EC, Di Bisceglie AM, Kim HY, Sterling RK, Everson GT, Lindsay KL, Lee WM, Bonkovsky HL, *et al*; HALT-C Trial Group: Maintenance peginterferon therapy and other factors associated with hepatocellular carcinoma in patients with advanced hepatitis C. Gastroenterology 140: 840-849, 2011.
13. Roberts SK, Therneau TM and Czaja AJ: Prognosis of histological cirrhosis in type 1 autoimmune hepatitis. Gastroenterology 110: 848-857, 1996.
14. Haudek SB, Xia Y, Huebener P, Lee JM, Carlson S, Crawford JR, Pilling D, Gomer RH, Trial J, Frangogiannis NG, *et al*: Bone marrow-derived fibroblast precursors mediate ischemic cardiomyopathy in mice. Proc Natl Acad Sci USA 103: 18284-18289, 2006.
15. Pilling D, Roife D, Wang M, Ronkainen SD, Crawford JR, Travis EL and Gomer RH: Reduction of bleomycin-induced pulmonary fibrosis by serum amyloid P. J Immunol 179: 4035-4044, 2007.
16. Phillips RJ, Burdick MD, Hong K, Lutz MA, Murray LA, Xue YY, Belperio JA, Keane MP and Strieter RM: Circulating fibrocytes traffic to the lungs in response to CXCL12 and mediate fibrosis. J Clin Invest 114: 438-446, 2004.
17. Murray LA, Chen Q, Kramer MS, Hesson DP, Argentieri RL, Peng X, Gulati M, Homer RJ, Russell T, van Rooijen N, *et al*: TGF-beta driven lung fibrosis is macrophage dependent and blocked by Serum amyloid P. Int J Biochem Cell Biol 43: 154-162, 2011.
18. Duffield JS and Lupher ML Jr: PRM-151 (recombinant human serum amyloid P/pentraxin 2) for the treatment of fibrosis. Drug News Perspect 23: 305-315, 2010.
19. Kisseleva T, Cong M, Paik Y, Scholten D, Jiang C, Benner C, Iwaisako K, Moore-Morris T, Scott B, Tsukamoto H, *et al*: Myofibroblasts revert to an inactive phenotype during regression of liver fibrosis. Proc Natl Acad Sci USA 109: 9448-9453, 2012.
20. Yang L, Roh YS, Song J, Zhang B, Liu C, Loomba R and Seki E: Transforming growth factor beta signaling in hepatocytes participates in steatohepatitis through regulation of cell death and lipid metabolism in mice. Hepatology 59: 483-495, 2014.
21. Iwaisako K, Haimerl M, Paik YH, Taura K, Kodama Y, Sirlin C, Yu E, Yu RT, Downes M, Evans RM, *et al*: Protection from liver fibrosis by a peroxisome proliferator-activated receptor δ agonist. Proc Natl Acad Sci USA 109: E1369-E1376, 2012.
22. Cong M, Liu T, Wang P, Fan X, Yang A, Bai Y, Peng Z, Wu P, Tong X, Chen J, *et al*: Antifibrotic effects of a recombinant adeno-associated virus carrying small interfering RNA targeting TIMP-1 in rat liver fibrosis. Am J Pathol 182: 1607-1616, 2013.
23. Cong M, Liu T, Wang P, Xu Y, Tang S, Wang B, Jia J, Liu Y, Hermonat PL and You H: Suppression of tissue inhibitor of metalloproteinase-1 by recombinant adeno-associated viruses carrying siRNAs in hepatic stellate cells. Int J Mol Med 24: 685-692, 2009.
24. Gredelj-Simec N, Jelić-Puskarić B, Ostojić A, Siftar Z, Fiala D, Kardum-Skelin I, Vrhovac R and Jaksić B: Diagnostic and prognostic significance of CD45 cell surface antigen expression in hematologic malignancies with main focus on acute leukemias. Acta Med Croatica 65 (Suppl 1): 45-52, 2011 (In Croatian).
25. Karakus E, Karadeniz A, Simsek N, Can I, Kara A, Yildirim S, Kalkan Y and Kisa F: Protective effect of Panax ginseng against serum biochemical changes and apoptosis in liver of rats treated with carbon tetrachloride (CCl_4). J Hazard Mater 195: 208-213, 2011.
26. Yang BY, Zhang XY, Guan SW and Hua ZC: Protective effect of procyanidin B_2 against CCl_4-induced acute liver injury in mice. Molecules 20: 12250-12265, 2015.
27. Ramm GA: Chemokine (C-C motif) receptors in fibrogenesis and hepatic regeneration following acute and chronic liver disease. Hepatology 50: 1664-1668, 2009.
28. Marra F, Romanelli RG, Giannini C, Failli P, Pastacaldi S, Arrighi MC, Pinzani M, Laffi G, Montalto P and Gentilini P: Monocyte chemotactic protein-1 as a chemoattractant for human hepatic stellate cells. Hepatology 29: 140-148, 1999.
29. Weber LW, Boll M and Stampfl A: Hepatotoxicity and mechanism of action of haloalkanes: Carbon tetrachloride as a toxicological model. Crit Rev Toxicol 33: 105-136, 2003.
30. Zhang F, Wang X, Qiu X, Wang J, Fang H, Wang Z, Sun Y and Xia Z: The protective effect of Esculentoside A on experimental acute liver injury in mice. PLoS One 9: e113107, 2014.
31. Spicer J, Brodt P and Ferri L: Role of inflammation in the early stages of liver metastasis. In: Liver Metastasis: Biology and Clinical Management. Brodt P (ed). Springer, pp155-185, 2011.
32. Kumar V, Abbas A, Fausto N and Aster J: Cellular Responses to Stress and Toxic Insults: Adaptation, Injury and Death. In: Robbins and Cotran Pathologic Basis of Disease. 8th edition. Saunders Elsevier, Philidelphia, pp18-19, 2009.
33. Canbay A, Taimr P, Torok N, Higuchi H, Friedman S and Gores GJ: Apoptotic body engulfment by a human stellate cell line is profibrogenic. Lab Invest 83: 655-663, 2003.
34. Zhan SS, Jiang JX, Wu J, Halsted C, Friedman SL, Zern MA and Torok NJ: Phagocytosis of apoptotic bodies by hepatic stellate cells induces NADPH oxidase and is associated with liver fibrosis in vivo. Hepatology 43: 435-443, 2006.
35. Jiang JX, Mikami K, Venugopal S, Li Y and Török NJ: Apoptotic body engulfment by hepatic stellate cells promotes their survival by the JAK/STAT and Akt/NF-kappaB-dependent pathways. J Hepatol 51: 139-148, 2009.
36. Watanabe A, Hashmi A, Gomes DA, Town T, Badou A, Flavell RA and Mehal WZ: Apoptotic hepatocyte DNA inhibits hepatic stellate cell chemotaxis via toll-like receptor 9. Hepatology 46: 1509-1518, 2007.
37. Castaño AP, Lin SL, Surowy T, Nowlin BT, Turlapati SA, Patel T, Singh A, Li S, Lupher ML Jr and Duffield JS: Serum amyloid P inhibits fibrosis through Fc gamma R-dependent monocyte-macrophage regulation in vivo. Sci Transl Med 1: 5ra13, 2009.
38. Murray LA, Rosada R, Moreira AP, Joshi A, Kramer MS, Hesson DP, Argentieri RL, Mathai S, Gulati M, Herzog EL, *et al*: Serum amyloid P therapeutically attenuates murine bleomycin-induced pulmonary fibrosis via its effects on macrophages. PLoS One 5: e9683, 2010.
39. Murray LA, Kramer MS, Hesson DP, Watkins BA, Fey EG, Argentieri RL, Shaheen F, Knight DA and Sonis ST: Serum amyloid P ameliorates radiation-induced oral mucositis and fibrosis. Fibrogenesis Tissue Repair 3: 11, 2010.
40. Haudek SB, Trial J, Xia Y, Gupta D, Pilling D and Entman ML: Fc receptor engagement mediates differentiation of cardiac fibroblast precursor cells. Proc Natl Acad Sci USA 105: 10179-10184, 2008.
41. Shen H, Zhang M, Kaita K, Minuk GY, Rempel J and Gong Y: Expression of Fc fragment receptors of immunoglobulin G (Fc gammaRs) in rat hepatic stellate cells. Dig Dis Sci 50: 181-187, 2005.
42. Blumberg RS, Koss T, Story CM, Barisani D, Polischuk J, Lipin A, Pablo L, Green R and Simister NE: A major histocompatibility complex class I-related Fc receptor for IgG on rat hepatocytes. J Clin Invest 95: 2397-2402, 1995.